



# Advances in microfluidic technology for sperm screening and in vitro fertilization

Jingtong Ma<sup>1</sup> · Qianlin Xie<sup>1</sup> · Yusongjia Zhang<sup>1</sup> · Qirui Xiao<sup>1</sup> · Xiaoyu Liu<sup>2</sup> · Chong Qiao<sup>3,4</sup> · Ye Tian<sup>1,5</sup>

Received: 2 November 2023 / Revised: 9 December 2023 / Accepted: 19 December 2023 / Published online: 8 January 2024  
© The Author(s), under exclusive licence to Springer-Verlag GmbH, DE part of Springer Nature 2024

## Abstract

About 18% of reproductive-age adults worldwide are affected by infertility. In vitro fertilization (IVF) and intracytoplasmic sperm injection (ICSI) are widely used assisted reproductive technologies (ARTs) aimed at improving clinical outcomes. Efficient and noninvasive selection and isolation of highly motile sperm with intact DNA are essential for the success of IVF and ICSI and can potentially impact the therapeutic efficacy and the health of the offspring. Compared to traditional methods, microfluidic technology offers significant advantages such as low sample consumption, high efficiency, minimal damage, high integration, similar microenvironment, and high automation, providing a new platform for ARTs. Here, we review the current situation of microfluidic technology in the field of sperm motility screening and evaluation and IVF research. First, we focus on the working principle, structural design, and screening results of sperm selection microfluidic platforms. We then highlight how the multiple steps of the IVF process can be facilitated and integrated into a microfluidic chip, including oocyte capture, sperm collection and isolation, sperm sorting, fertilization, and embryo culture. Ultimately, we summarize how microfluidics can complement and optimize current sperm sorting and IVF protocols, and challenges and possible solutions are discussed.

**Keywords** Microfluidics · Sperm screening · In vitro fertilization (IVF) · Assisted reproductive technologies (ARTs) · Intracytoplasmic sperm injection (ICSI)

## Introduction

Infertility is defined by the World Health Organization (WHO) as “a disease of the reproductive system defined by the failure to achieve a clinical pregnancy after 12 months or more of regular unprotected sexual intercourse” [1]. Infertility impacts millions of people worldwide, often with grave consequences. According to data from 1990 to 2021, about one in six people in the world have experienced infertility, and the global lifetime prevalence of infertility is estimated to be about 18% in 2022 [2]. In these cases, about 60% of cases are the result of low sperm concentration (oligospermia), poor sperm motility (azoospermia), and abnormal sperm morphology (teratozoospermia) [3]. Many of these cases must be treated with assisted reproductive techniques (ARTs), such as in vitro fertilization (IVF), intracytoplasmic sperm injection (ICSI), and intrauterine insemination (IUI) [4, 5].

The most typical ART methods are IVF and ICSI [6]. The IVF technology uses hormones to stimulate the ovaries to expel the eggs. Next, mature oocytes are extracted from

✉ Xiaoyu Liu  
328609292@qq.com

✉ Chong Qiao  
qiaochong2002@hotmail.com

✉ Ye Tian  
tianye@bmie.neu.edu.cn

<sup>1</sup> College of Medicine and Biological Information Engineering, Northeastern University, Shenyang 110169, China

<sup>2</sup> Department of Obstetrics and Gynaecology, General Hospital of Northern Theater Command, Shenyang 110003, China

<sup>3</sup> Department of Obstetrics and Gynecology of Shengjing Hospital of China Medical University, Shenyang 110022, China

<sup>4</sup> Key Laboratory of Maternal-Fetal Medicine of Liaoning Province, Shenyang 110022, China

<sup>5</sup> Foshan Graduate School of Innovation, Northeastern University, Foshan 528300, China

the patient's ovary and fertilized with sperm in the laboratory. The zygote is subsequently implanted into the patient's uterus. During conventional IVF, each oocyte is placed in an oil-covered microdroplet in the optimal concentration of sperm, and is fertilized when a sperm penetrates the oocyte in a natural way. But when couples with defective sperm quality and quantity are unable to undergo the IVF process, it is necessary to introduce ICSI. ICSI is a precise technique that injects a sperm directly into the cytoplasm of the oocyte using a fine needle under a microscope. ICSI is the primary treatment method for almost all male infertility, and it is also increasingly used to overcome fertilization-in-failure [7]. By 2006, more than three million infants around the world were conceived through either IVF or ICSI [8]. In 2016, a total of 197,706 IVF procedures aiming to transplant at least one embryo were performed in the United States and 76,892 babies were born through these techniques, almost 1.8% of all newborn births in the United States [9]. The use of these types of ART continues to increase as the growth of infertility problems due to environmental contamination, diet, smoking habit, and various other causes.

Although ART has great potential to solve the problem of infertility, there are still many limitations associated with traditional ART systems. First, this technique relies heavily on the skill level and experience of operators and lacks technical standards [10]. Moreover, the lack of effective *in vitro* sperm selection methods for ARTs is considered to be one of the relatively low pregnancy rates achieved in human clinical practice by procedures such as ICSI [11]. Thus, developing a selection method capable of screening out sperm with high viability and high DNA integrity is a major challenge for ARTs, especially of ICSI [12, 13]. In clinical practice, several methods have been developed for the sperm preparation before ARTs [14], and the swim-up method (SU) and density gradient centrifugation (DGC) are the most common screening methods [15]. Nevertheless, these methods are quite different from the multiple screening mechanisms *in vivo*, and the length of time and too much centrifugation can easily lead to sperm DNA peroxidation damage and sperm breakage, resulting in a decrease in the pregnancy success rate [16]. More importantly, conventional IVF and ICSI bypass natural selection processes and the *in vivo* reproductive tract environment [13]. In spite of the fact that there are significant improvements in gamete processing and culture medium of simulating *in vivo* conditions based on the embryo need, it is difficult to simulate real dynamic microenvironments *in vivo* only by utilizing physical tools such as test tubes, culture dishes, microdroplets, and micropores alone. It may adversely affect fertilization success rate, embryo quality, and pregnancy rate, but also epigenetics in offspring.

The technical limitations of traditional methods can be overcome by combining miniaturization and automation

techniques rapidly developed in recent decades, such as microfluidic technologies. In the biomedical field, microfluidics is widely used in clinical diagnostics and *in vitro* biomimetic models. Microfluidic technology has the advantages of low sample consumption, low cost, and short reaction time in a fast, efficient, traceable, and sensitive manner [17]. In addition, the miniaturization and automation provided by microfluidics can further improve experimental accuracy, reduce detection limitations, and enable the development of techniques and experiments [18] that are impossible at the macro-scale. Although it is impossible to fully replicate all of the features of the oviduct environment in sperm sorting, some features, such as unidirectional and laminar or gradient flow, can be achieved in a microfluidic environment. Based on the above characteristics, microfluidic techniques can be used in ARTs to overcome the technical limitations of conventional methods. Over the past 30 years, microfluidic technologies have shown great potential for sperm screening and simplifying the IVF process [19]. In this review, we summarize the progress of microfluidic technology in the fields of sperm motility (the percentage of progressive motion of spermatozoa in the semen) screening, evaluation, and IVF chip. This paper first reviews the representative sperm sorting chips, including manufacturing materials, sorting mechanisms, structural design, and screening results. Subsequently, we focused on how microfluidic techniques can achieve the functional integration of sperm sorting, oocyte localization, continuous fertilization, and embryo culture within an IVF chip. Then, we analyze the advantages and limitations of these methods, and provide some suggestions for improvement and innovation. Finally, the future direction of the microfluidics of ARTs is discussed. This review aims to stimulate new advances in the application of microfluidic technologies in ARTs, motivating more researchers and clinicians to increase the practice of using microfluidic techniques to treat infertility.

## Screening of Motile Sperm on a Chip

Sperm have to swim thousands of body lengths in the complex environments of the female reproductive tract to achieve fertilization, but details of how sperm migrate through the female reproductive tract are largely unknown [20]. As the most promising method for biomimetic sperm selection, microfluidics is able to realize the interaction mechanisms of the different geometry, fluid, chemical environment, and temperature with the female reproductive tract by reconstructing the natural *in vivo* environment. Current microfluidic technologies for sperm sorting are summarized in Table 1. In this section, we will discuss the selection mechanism, structural design and manipulation, and sorting results of different microfluidic sperm sorting platforms.

**Table 1** Current microfluidic techniques for sperm sorting

| Principle                  | Chip materials                          | Sperm type         | Amount of sample   | Time                  | Motility/Vitality                 | DFI                                 | Refs |
|----------------------------|---|--------------------|--|-----------------------|-----------------------------------|-------------------------------------|------|
| Microchannel               | PDMS, PMMA                              | Bull, human        | 1 mL raw semen (over 50 million sperm)                           | 10–20 min             | 89–96%                            | 2.40–4.32%                          | [21] |
| Microchannel               | PDMS                                    | Human              | 200 $\mu$ L raw semen  | 15 min                | $88.8 \pm 4.3\% - 93.6 \pm 1.6\%$ | $1.16 \pm 0.39\% - 1.63 \pm 0.79\%$ | [22] |
| Microchannel               | PDMS, silicon, glass                    | Human              | NA   | 5, 10, 20, and 30 min | $\approx 99\%$                    | 4–6%                                | [23] |
| Microchannel               | NA                                      | Human              | 100 $\mu$ L raw semen  | 10 min                | $> 97\%$                          | 2.6–2.8%                            | [24] |
| Microchannel               | PDMS                                    | Zebrafish          | 3 $\mu$ L sperm solution   | NA                    | 80%                               | NA                                  | [25] |
| Laminar flow               | PDMS                                    | Human              | 50 $\mu$ L washed semen sample                                   | 20 s                  | $\approx 100\%$                   | NA                                  | [26] |
| Laminar flow               | Cycloolefin polymer                     | Human              | 65 $\mu$ L of sperm suspension ( $300 \times 10^3$ sperm)        | 30 min                | $95.4 \pm 3.0\%$                  | $0.8 \pm 1.9\%$                     | [27] |
| Laminar flow               | PDMS, silicon                           | Boar               | NA   | 1–2 min               | $\approx 80\%$                    | NA                                  | [28] |
| Rheology                   | PDMS,                                   | Bull, mouse, human | 20 $\mu$ L semen sample  | 20 min                | 78.8%                             | NA                                  | [29] |
| Rheology                   | PDMS                                    | Human              | 2,000,000 sperm (10 $\mu$ L of sperm suspension)                 | 20 min                | 90%                               | NA                                  | [30] |
| Rheology                   | PMMA, PDMS                              | Bull               | $\leq 1$ million sperm   | 30 min                | $\approx 100\%$                   | 0.37%                               | [31] |
| Rheology                   | PDMS                                    | Human, bovine      | 250 $\mu$ L semen solution (1:1 diluted sample)                  | 12–45 min             | $\approx 100\%$                   | NA                                  | [32] |
| Chemotaxis                 | PDMS, glass                             | Mouse              | 50 $\mu$ L sperm sample  | 1 h                   | NA                                | NA                                  | [33] |
| Chemotaxis                 | PDMS, glass                             | mouse              | 1 $\mu$ L sperm sample   | 10 min                | $\approx 100\%$                   | NA                                  | [34] |
| Chemotaxis                 | NA                                      | Human              | 130 $\mu$ L sperm suspension                                     | 20 min                | $\approx 80\%$                    | NA                                  | [35] |
| Chemotaxis                 | Polystyrene                             | Human              | 200 $\mu$ L sperm suspension                                     | 150 min               | $\approx 100\%$                   | $6.8 \pm 3.3\%$                     | [36] |
| Chemotaxis                 | Hybrid hydrogel (8% gelatin/1% agarose) | Boar               | 0.5 $\mu$ L of sperm solution ( $20 \times 10^6$ spermatozoa/mL) | 20 min                | 2.4%/min                          | NA                                  | [37] |
| Thermotaxis                | PDMS                                    | Human              | 0.5 mL sperm sample ( $2.5-20 \times 10^3$ sperm)                | 15 min                | NA                                | NA                                  | [38] |
| Thermotaxis                | NA                                      | Mouse, human       | $1 \times 10^6$ mouse sperm and $3-10 \times 10^6$ human sperm   | 1 h                   | $\approx 100\%$                   | $3 \pm 2\%$                         | [39] |
| Chemotaxis and thermotaxis | PDMS, glass, ITO                        | Mouse              | 1 $\mu$ L sperm sample   | 13 min                | NA                                | NA                                  | [40] |
| Chemotaxis and thermotaxis | PDMS, glass, ITO                        | Human              | 20 motile sperm  | 1 h                   | NA                                | NA                                  | [41] |

DFI, DNA fragmentation index; PDMS, polydimethylsiloxane; PMMA, polymethylmethacrylate; ITO, indium tin oxide.

### Screening of sperm by microchannels

The first attempt in this area was performed to screen the sperm on a microfluidic chip using a silicon glass

microtubule chip, demonstrating the feasibility of this approach [42, 43]. A series of experiments was performed to show that sperm can effectively pass through a single continuous pipes of different widths, branch cascade pipes,

and curved pipes, which showed that there is a correlation between the motility scores (forward progression score, determined based on the time required for sperm to reach the ends of different microchip channels) and the distance the first sperm travels in the chip. Since this technique allows motility of sperm to be determined in a single direction, it is able to reduce the subjectivity of conventional approaches such as microscope slides, Markler chambers or computer-aided sperm analysis (CASA). Sperm screening through the straight channel is fast and simple, but there is no universally accepted size standard. Xie et al. [44] used the relative number of sperm and sperm motility as the evaluation criteria to verify the screening effect of a straight channel by fluorescent labeled sperm. Finally, they found that a pipeline 7 mm long, 1 mm wide, and 100  $\mu\text{m}$  deep had the best motility screening effect for mouse sperm, and the optimal screening time was between 15 and 30 min.

Denissenkoa et al. [45] studied the behavior of sperm in curved microchannels with a cross-section similar to the

fallopian tube structure. They found that sperm cells rarely swim in the center of the microchannel, but rather in the channel corners. Sperm swimming against the walls due to the conical envelope of the flagella wave are larger than the amplitude of head oscillations, which leads to propulsion toward the wall. Sperm changing their spatial orientation by following the boundary wall surface interaction is known as boundary-following navigation. In this regard, Nosrati et al. [21] proposed a microchip that selected sperm based on progressive motility with 500 microchannels (Fig. 1a). The device contains two layers; the bottom consists of 500 radial arrays of upfacing microchannels, while the top has a removable top seal to ensure a flow-free environment. The microchannel size of the device (100  $\mu\text{m}$   $\times$  75  $\mu\text{m}$ ) depends on the distance between the ciliated epithelium of the fallopian tube and the average length of the human sperm, triggering the boundary-following of the sperm [45]. Over 50 million sperm from 1 mL of raw semen can be processed within 10–20 min. Compared with conventional methods,

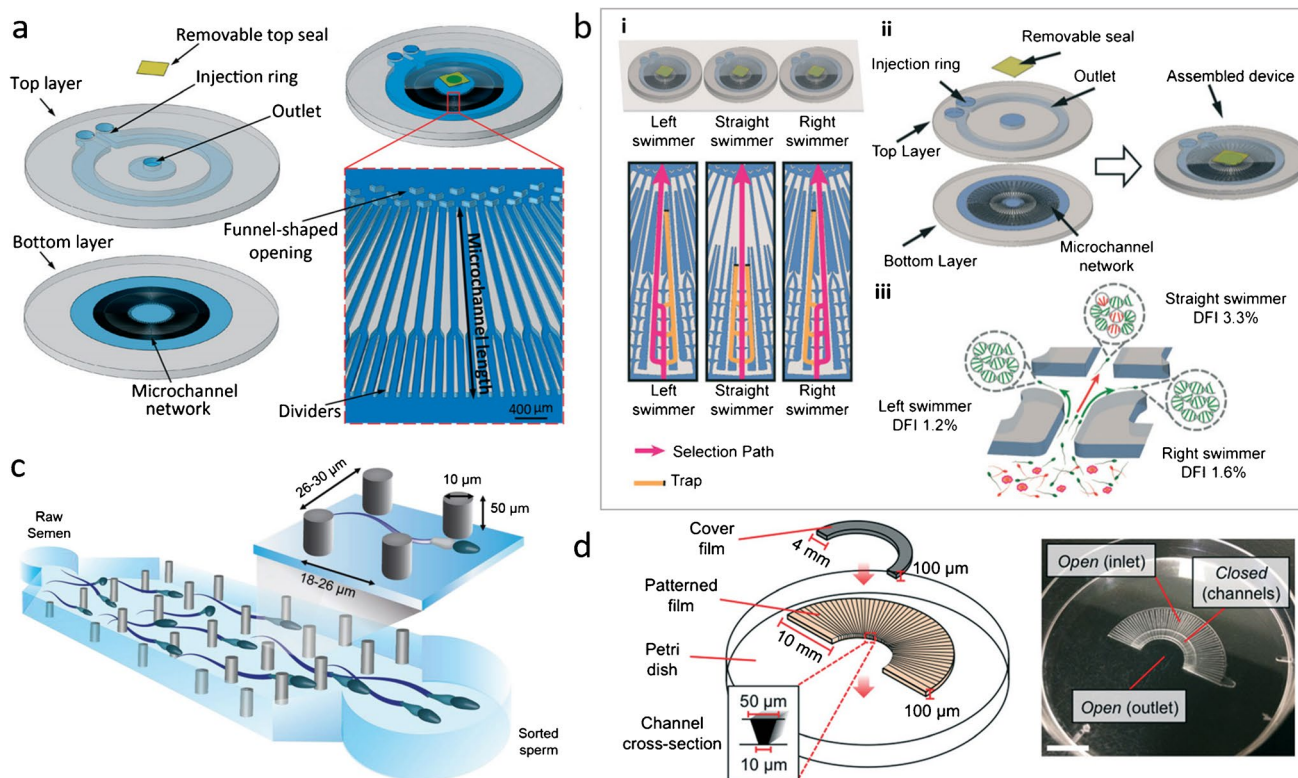


**Fig. 1** Microfluidic chip system for sperm selection based on microchannels. **a** A microfluidic sperm selection device with capacity for 1 mL of raw semen based on 500 parallel microchannels. Reproduced with permission [21], Copyright © 2014, RSC Publishing. **b** Schematic diagram of a passive microfluidic device for sperm separation based on the boundary-following behavior. (i) Three different structures of microfluidic system, including straight swimming path, left swimming path, and right swimming path. (ii) Inlets and outlets of the device containing 52 microchannels each 7.0 mm  $\times$  100  $\mu\text{m}$   $\times$  60  $\mu\text{m}$  in size. (iii) Schematic of sperm swimming toward the out-

let showing that only live sperm are able to navigate from the inlet towards the outlet, and the left and right swimming sperm had lower DFI than the straight swimming sperm. Reproduced with permission [22], Copyright © 2016, RSC Publishing. **c** SPARTAN (Simple Periodic ARray for Trapping And isolationN) for selecting sperm with normal motility and morphology. Reproduced with permission [23], Copyright © 2018, PNAS Publishing. **d** Schematic diagram of Fert-Dish, comprising a two-layer film (a combination of a cover film and a patterned film) and a standard ICSI Petri dish [24], Copyright © 2021, RSC Publishing

experiments with bull sperm showed that selected sperm vitality (the percentage of live spermatozoa in the semen) was increased by more than 89%; clinical trials of human sperm showed that sperm DNA integrity was improved by more than 80%. In another experiment, Eamer et al. [22] also fabricated three radial microfluidic devices with 52 microchannels to collect motile sperm based on their preference to follow boundaries and turn corners (Fig. 1b). Each chip had a specific channel configuration, allowing for the collection of sperm with preferences to follow the boundaries on the left-hand side, right-hand side, or to swim straight, respectively. They found a significant correlation between high DNA integrity and the propensity of sperm to follow boundaries. The data showed that human sperm exhibit a clockwise flagellar wave and they are prone to turn left when near the bottom boundary wall and right when near the top boundary wall. Sperm swimming along the right-hand-side and left-hand-side boundary walls showed more than 51% and 67% DNA integrity, which was higher than the DNA integrity of the straight swimmers. Additionally, a sperm motility screening model with microfluidic channels, named SPARTAN (Simple Periodic ARray for Trapping And isolation) [23] was developed (Fig. 1c). Sperm swimming behavior in the periodic column array geometry was simulated using rectangular arrays with spacing values of  $18 \times 26$ ,  $22 \times 22$ ,  $22 \times 26$ ,  $26 \times 26$ , and  $30 \times 26$   $\mu\text{m}$ . Sperm with morphological defects failed to efficiently pass through channels due to their abnormal motility properties, so sperm with normal motility and morphology (a set of criteria whereby sperm must fit within specific measurements and lack defects, including acrosome defects, head defects, midpiece abnormalities, and tail defects) can be effectively separated from sperm with low epigenetic global methylation. The device can separate motile sperm from non-motile sperm in just 10 min and the sorted sperm motility was over 99%, the morphology was improved by five times, the nuclear maturity was increased by three times, and the DNA integrity was enhanced by 2–4 times. Recently, Xiao et al. [24] presented a microfluidic sperm selection-in-a-dish platform, FertDish (Fig. 1d). It contained a two-layer film featuring an array of 60 sperm-selective microchannels which utilized the boundary-following behavior to select sperm directly from raw semen. The FertDish format mimicked the clinically established ICSI dish setup, and provides rapid (<10 min) single stage sperm preparation, supporting all sperm preparation, processing steps and ICSI in-dish. Sperm selected from the FertDish showed a significant improvement in DNA quality over the original semen, characterized by a DNA fragmentation index (%DFI, a measure of DNA strand breaks) of over 91% (donor) and 74% (patient), and more than 97% of sperm with vigorous and high levels of DNA. FertDish also had a high sperm recovery rate (the ratio of the number of motile sperm in the outlet to the total number of motile

sperm in the sperm sample inlet), which totally satisfied the ICSI standard. The FertDish efficiently selects high-quality sperm in a clinically adaptable manner, with the potential to improve the economy and effectiveness of ICSI.

It is remarkable that microchannel-based microfluidics could also be used for high-quality sperm sorting in the fish. This is because the sperm of some marine animals, such as zebrafish, do not follow physical and chemical guidance mechanisms, such as temperature gradients, chemical concentration gradients, or rheological behavior, to reach the egg [46]. Hence, a microfluidic concept based on PDMS baffle can be used to collect zebrafish sperm after state activation [25]. The geometric microconstraints of the baffle array produced a series of flow contraction and expansion regions. Due to the loss of fluid momentum, the expansion region created a flowless region near the sidewall, while the sperm tended to swim towards microscale confinement and were trapped there. Two baffle designs were further tested to effectively retain the sperm, and they observed that the baffle design as the letter J structure performed better in sperm extraction. The results showed that the device achieved 44% improvement in sperm recovery efficiency. It was further observed that 80% of the total sperm population could swim into the retention zones when the fluid rate was optimized to 0.7  $\mu\text{L}/\text{min}$ . This study further paves the way for developing the practice of IVF of fish.

Microchannel sperm screening technology is easy to operate without worrying about the stability of the system and is therefore user-friendly. At the same time, adding some viscoelastic medium similar to the female reproductive channel in the microchannel can better simulate the natural preferred process of sperm in a real physiological environment. For example, a recent study of microchannels has revealed how highly motile sperm can compete for oocyte fertilization in vivo [47]. To some extent, this could be a biomimetic device based on sperm autonomous movement, so its clinical application prospect is very broad, whereas relying solely on motility properties and size to classify and select sperm by microfluidic technology is obviously not a comprehensive assessment of sperm quality. There have been a number of further innovations in these systems by adding chemoattractants or temperature gradients [33–37, 39–41, 48, 49]. Moreover, their complex design seriously increases the fabrication cost, causing obstacles in mass production in the clinical stage.

### Screening of sperm by laminar flow effect

The microchannel of the microfluidic chip allows multiple laminar streams to flow parallel to each other, and there is no turbulent mixing at the interface between the laminar streams [50–52]. The flow of semen and media were mixed independently and parallelly through diffusion due to the

nature of the laminar flow. Motile sperm have a higher diffusion rate, allowing them to swim across the streamline in a laminar flow field. Eventually, nonmotile sperm flowed out from one outlet along their initial streamline, while motile sperm deviated from their original streamline and flowed out through another outlet.

Cho et al. reported a microscale integrated sperm sorter (MISS) based on laminar flow effects for the first time. The MISS (Fig. 2a, b) [26] takes advantage of active movement of cells, allowing for efficient collection of only the motile sperm that deviate from their initial inlet stream. After

sorting using this device, the percentage of motile sperm was nearly 100%, and the normal morphology rate was increased from  $9.5 \pm 1.1\%$  to  $22.4 \pm 3.3\%$ . Later, a clinical test of a similar device showed a significantly lower rate of selected sperm DNA fragmentation compared to centrifugation and swim methods [27]. Although the screening results of these devices were relatively satisfactory, the sperm recovery rate and efficiency of these sperm sorter devices were low, and their use also had some limitations. For example, during the sorting process, the pressure must be stable and the flow rate has

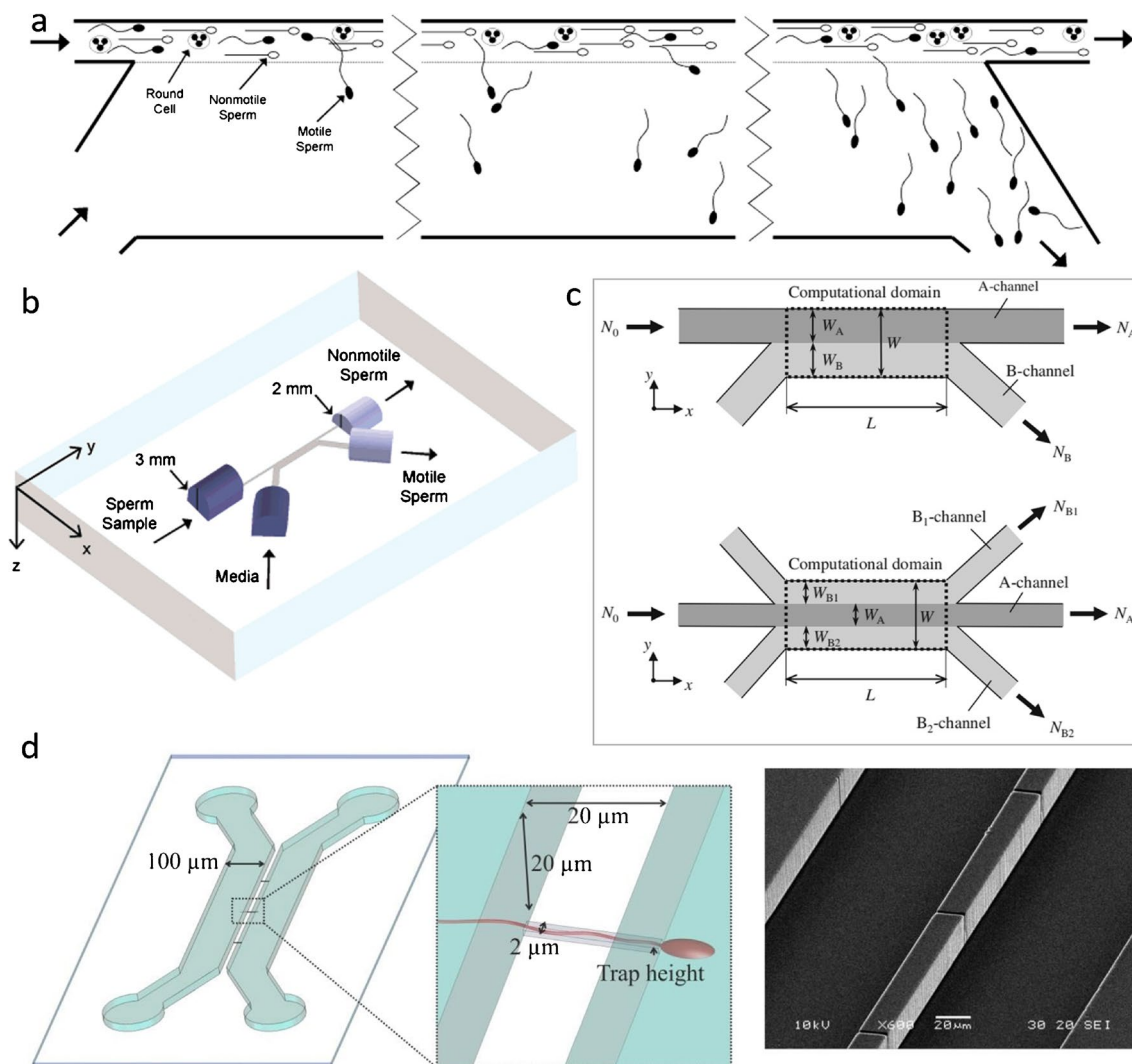


**Fig. 2** Microfluidic chip system for sperm selection based on laminar effect. **(a–b)** A compact, simple, disposable passive driving sperm sorting device. **a** A schematic figure of sperm sorter. Fluid containing sperm flows in from the inlet, and immobile sperm and cells reach the outlet along the initial stream. However, some motile sperm reach another outlet through the interface. **b** Three-dimensional geometrical depiction of the two-inlet, two-outlet microfluidic channel designs with horizontally oriented fluid reservoirs that serve as passively driven, steady-flow rate pumps. Reproduced with permission

[26], Copyright © 2003, ACS Publishing. **c** Sperm sorting chip based on the ability of motile sperm to cross streamlines in a laminar fluid stream. Two-inlet, two-outlet microfluidic channel and three inlet, three-outlet microfluidic channel. Reproduced with permission [53], Copyright © 2009, Springer Publishing. **d** A microfluidic platform for single-sperm entrapment. It consists of two main channels (width 100  $\mu\text{m}$ , height 20  $\mu\text{m}$ ) and 20 side channels (width 2  $\mu\text{m}$ , length 20  $\mu\text{m}$ ) that connect the main channel. Reproduced with permission [28], Copyright © 2015, RSC Publishing

to be large enough to prevent the sperm from swimming in opposite directions. To improve the separation efficiency of a sperm sorter, the application of numerical simulations can improve the separation efficiency of microfluidic sperm sorters [53], which analyzed how the changes in the height of the microchannel and the width of the sperm-inlet channel affected the number of active sperm extracted from outlet channel B (Fig. 2c). The results showed that the fluid velocity in the channel was a direct factor affecting the screening rate. For the two-inlet and two-outlet configuration, when  $W_A/W=0.25$  (where the width of the A-channel is  $W_A$  and that of the whole microchannel is  $W$ ), the microchannel height had little influence on the number of motile sperm reaching channel B. When the height was constant, the separation efficiency of motile sperm decreased with the increase in  $W_A/W$ . In addition to the existing double-inlet and double-outlet microfluidic channels, the three-inlet and three-outlet microfluidic channel systems were also analyzed. Because the flow rate of channel A in the three-inlet and three-outlet microfluidic channel was faster than that in the double-inlet and double-outlet microfluidic channel, the screening rate of high motile sperm increased significantly. Compared to population-based sperm selection techniques, some reports focused on the manipulation and separation of sperm at the single cell level. de Wagenaar et al. [28] proposed a flow graph dynamics-based microfluidic platform for capturing and selecting a single sperm with two main microchannels and a series of connected side channels (Fig. 2d). The flow rate of the main channel ( $0.025 \mu\text{L}/\text{min}$ ) containing sperm was lower than that of each side channel ( $2.5 \mu\text{L}/\text{min}$ ), resulting in pressure-driven flow in the side channels, pulling and trapping individual sperm in each side channel. This platform allows for noninvasive analysis of sperm at single cell level (viability, chromosome content and acrosome status) and has the potential to become a multifunctional tool for sperm selection application or basic research. Furthermore, this microfluidic single-sperm selection approach is a potential alternative to conventional methods for sperm selection in ICSI.

The laminar effect-based sperm motility screening chips leverage hydrostatic pressure and capillary forces to precisely control the flow, eliminating the need for external pumping systems and support equipment. After screening by this technique, there is a significant improvement in sperm motility, and it is able to minimize the damage to the sperm DNA. However, several important problems in such approaches need to be addressed. For instance, the sample size of semen that such devices can handle at a time is generally small and sorting efficiency and sperm recovery are relatively low, so the clinical application of this technique is still limited. To improve the efficiency of sperm sorting, the throughput of the device can be augmented by incorporating

multiple entrances and outlets or by widening the main sorting channel.

## Screening of sperm by rheology

Rheology, is the ability of cells and organisms to swim in a specific orientation within a fluid flow gradient. Positive rheology refers to the tendency of cells to swim against the direction of flow [54]. Between the fallopian tube and the uterus, the sperm can show a positive rheology to guide them to swim upstream towards the oocyte. Contrary to short-range mechanisms, such as chemical or temperature gradients, rheology is considered to be the key mechanism of long-range sperm guidance in the mammalian reproductive tract. The classification depends on the ability of the sperm themselves to swim out of the liquid fluid and pass through the microchannels, reducing the risk of injury.

A fluid static-drive [29] was fabricated to classify sperm in the microchannel based on their movement in the upstream direction, which consisted of four channels and three reservoirs (Fig. 3a, b). These four passages converged at a “junction”. The height of the liquid column in reservoir 1 generated the hydrostatic pressure to drive the flow, reservoir 2 contained sperm to be classified, and reservoir 3 collected classified sperm. Motile sperm were able to reach the junction against the fluid in the B channel and then were transported to reservoir 3 by high-speed fluid to achieve sperm optimization. Using this method to sort three bull sperm samples, the sperm motility was increased from an average of 18.4% to 78.8%. Wu et al. [30] designed a microfluidic device capable of generating a delayed flow field to classify and separate human motile sperm in a high-throughput manner (Fig. 3c). They proposed the flowing upstream sperm sorter (FUSS), which consisted of a diffusive sperm sorter capable of distinguishing sperm with varying motility by analyzing the rheology of human sperm in a delayed flow field. Then, the non-motile sperm were processed through the dumbbell flow field into the exit to be separated from the motile sperm. The aim was to simulate the selection mechanism that occurs in a woman’s body when sperm swim into the uterus. The FUSS chip was capable of processing sperm concentrations of up to 200 million cells per milliliter, sorting 95% of mobile sperm and approximately 20% of sperm over  $120 \mu\text{m}/\text{s}$ . In addition, a diffusion microfluidic sperm sorter (DMSS) [31] was developed for selecting functional and progressively motile bovine spermatozoa (Fig. 3d), which were separated via a crescent diffuser zone, a flow channel with a gradually expanding cross-section, and multiple channels. As the width of the crescent zone increased, the velocity weakened. The sperm acquired rheology when their moving velocity matches the velocity of the fluid, thus causing them to separate at different specific locations along the diffuser. Then, progressively motile sperm reached the

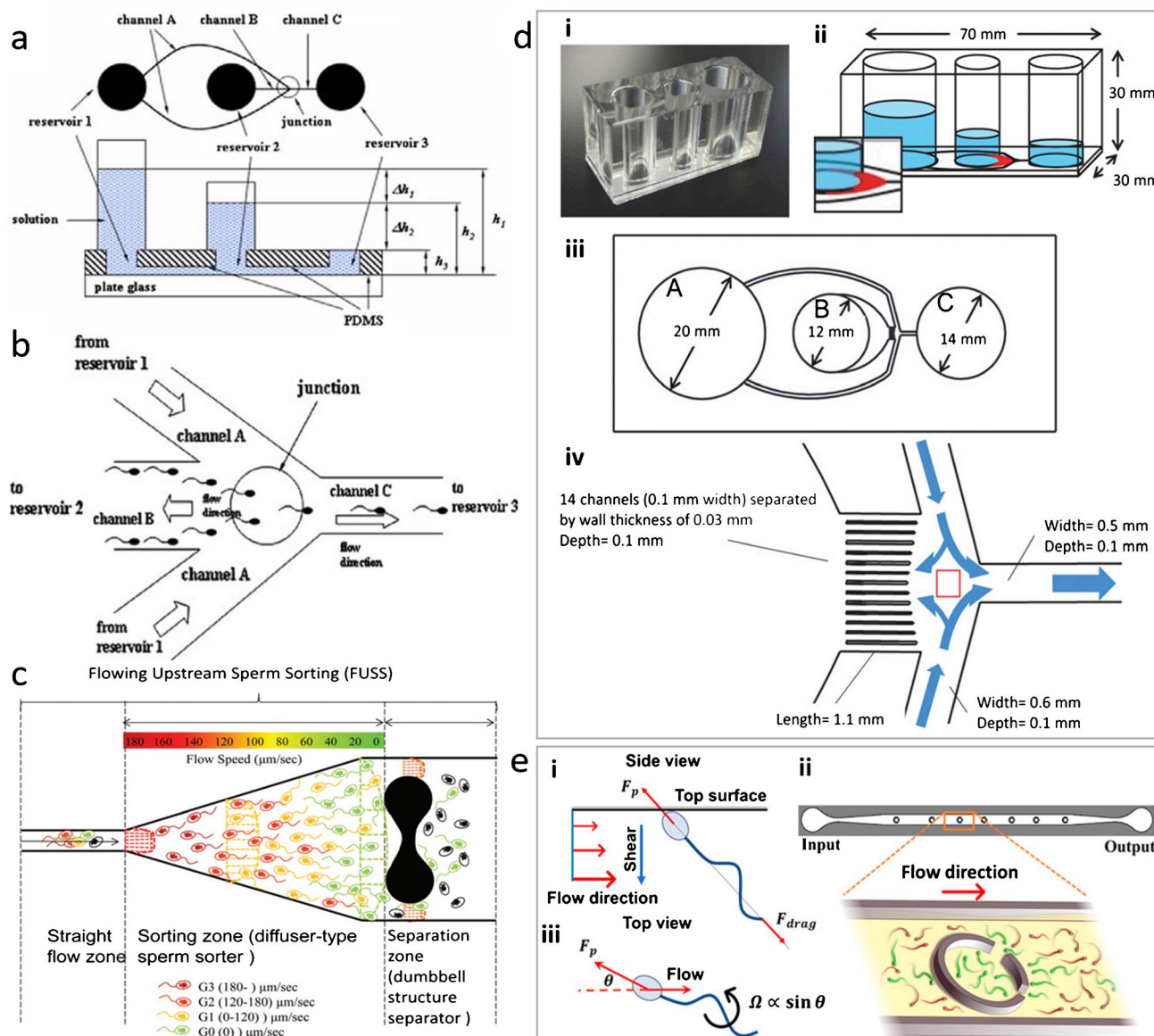


**Fig. 3** Microfluidic chip system for sperm selection based on rheology. (a–b) Design of the motile sperm sorting microfluidic system (MSMS). **a** Side view of the device and schematic of the generation of hydrostatic pressure differences. **b** Junction showing sperm movement from input (reservoir 2) to outlet (reservoir 3). Reproduced with permission [29], Copyright © 2007, Springer Publishing. **c** Design of the flowing upstream sperm sorter (FUSS) microchip. Reproduced with permission [30], Copyright © 2017, RSC Publishing. **d** Design of a diffusion microfluidic sperm sorter (DMSS). (i) Photograph of the device composed of PDMS and glass. (ii) Microchannels and

chambers A, B, and C. The crescent shape diffuser is shown in red. (iii) Microchannel design and geometry from the bottom view of the device. (iv) Magnified illustration of the 14 microchannels each separated by a channel wall and the junction area shown as the red square. Reproduced with permission [31], Copyright © 2018, PNAS Publishing. **e** Minimal hydrodynamic model for the upstream orientation of sperm. (i) Side view of the sperm in the vicinity of the top surface. (ii) Top view of the sperm. (iii) PDMS microfluidic device featuring seven corrals inside a flow channel. Reproduced with permission [32], Copyright © 2018, PNAS Publishing

entrance of multiple channels and were provided a preferential channel based on their swimming speed. Only a few high-quality sperm would navigate forward along the center of the channels to the junction, where they were gently swept into the chamber C (collection chamber). It has been proven that sperm selected using DMSS achieved 100% viability and mobility and increased DNA integrity by over 95%.

The proportion of capacitated sperm increased from 43% to 63% and the mitochondrial activity increased from 60% to 98%. The two main features of this microchip are the crescent diffuser and the multi-channel design. The area of the diffuser expands, thus gradually reducing the flow rate. This increase in throughput is the first stage of filtration for the device, while multiple channels not only improve the



sorting efficiency but also enhance the quality of the sorted sperm. Then, a method based on the rheological behavior of sperm was proposed to separate motile human and cattle sperm with corral features within microfluidic channels [32] (Fig. 3e). The finite element method (FEM) simulations showed that controlling a certain flow rate can create a rheological zone before the corral. The inactive sperm can only move along the streamline, but normal and surviving sperm can swim upstream of the corral until they enter the corral to be captured. This microfluidic device can limit the movement speed of human and cattle sperm samples within the range of 48 to 93  $\mu\text{m/s}$  and 51 to 82  $\mu\text{m/s}$ , respectively. More importantly, the isolated fraction of the human and cattle samples had 100% normal progressive motility. Moreover, by analyzing the distribution of sperm swimming in the rheological zone and the velocity distribution of sperm in the corral, researchers discovered that the motility of the separated samples could be modified by altering the flow rate.

In conclusion, microfluidics provide a highly controlled platform for studying the rheology of sperm in physiological environments, and microfluidic systems based on sperm rheotaxis are of great relevance to selecting functional sperm effectively. However, it should be noted that maintaining a stable upstream stream within it is challenging, especially in the clinical stage. The use of hydrostatic pressure instead of a syringe pump system is currently an effective solution.

### Screening of sperm by chemotaxis and thermotaxis

Within the mammalian female reproductive tract, only about 10% of the ejaculated sperm reach maturity through a process called capacitation. They typically have better cell morphology, sperm motility, maturity, and DNA integrity [55], which gives them the ability to fertilize the oocyte. Of several sperm guidance mechanisms, only two react exclusively on capacitated spermatozoa: chemotaxis and thermotaxis, as short-term guidance mechanisms acting within the ampullary region close to the oocyte [56]. Therefore, chemotaxis and thermotaxis can be viewed as mechanisms for selecting capacitated and thus optimal spermatozoa to fertilize the oocyte.

Sperm chemotaxis refers to the movement of sperm cells in response to a concentration gradient of a chemotactic agent. Spermatozoa are attracted to cytokines released from the oocyte and are able to navigate within the short-range inward fertilization site through chemotaxis [57]. The main chemoattractants in the reproductive tract are progesterone and atrial natriuretic titanium, secreted by the cumulus cells of the ovulating oocytes [58, 59]. The chemotaxis of mouse sperm to ovarian extract was first evaluated on a chip [33] (Fig. 4a). The injection channels were filled into ovarian extract, mouse semen and buffer, and a chemical gradient was formed in the intersectional micro-cavity. The

experimental results showed that about 7% of mouse sperm had chemotaxis ability. In another study, acetylcholine was used as a chemoattractant to investigate the chemoattractant properties of sperm [34]. This study showed that progressive motile sperm swam mostly toward the outlet at an optimal chemical gradient of 0.625 (mg/mL)/mm of acetylcholine. A microfluidic device with two wells connected by a fluidic channel was developed by Gatica et al. [35] One well was filled with sperm suspension and the other with picomolar progesterone and spread in a gradient in the connecting tube (Fig. 4b). After the sperm selection assay, the mean level of capacitated sperm increased threefold in normal and subfertile samples, and sperm levels with intact DNA fortified significantly, while sperm oxidative stress levels decreased. To improve the mimicking of the chemotaxis mechanism, a hexagonal microchamber connecting six microchannels [48] (Fig. 4c) was designed. The device allows for three parallel experiments on the same chip and deepens the study of sperm chemotaxis. The chemokinetic response of sperm was assessed leveraging actual curvilinear path, straight path and the linearity of the trajectory. They observed sperm behavior at two progesterone concentration gradients (100 pm and 1 mm, respectively), and the result showed that sperm became more hyperactive at this concentration of progesterone. The advantage of this system is the use of a multi-channel gradient on the chip, which helps to reduce experimental errors and save time in experiment. Li et al. [36] designed a novel distance-progesterone-combined selection chip inspired by the human female reproductive tract (Fig. 4d). The device included three chambers that mimic the anatomy of the human female reproductive organs, including a vagina and two ovaries. The channel between Chambers F and G simulated the fallopian tube, and its central Position C simulated the uterus. The setting at the bottom of the channel between F and G maintained the agar mixed with the chemotactic groove to form the gradient. Two hundred microliters of treated sperm was added to Chamber A and allowed to swim for 150 min. Finally, the sperm at the D2 and E2 grooves were collected to assess their morphology and DNA integrity. After sperm were selected, the portion of sperm with regular morphology increased from  $11.2 \pm 1.3\%$  to  $40.3 \pm 6.6\%$ , and the portion of sperm with DNA fragmentation decreased from  $15.4 \pm 4.0\%$  to  $6.8 \pm 3.3\%$ . Recently, Berendsen et al. [37] designed a simple, easy to manufacture and process, flowless microfluidic chip based on hydrogel. The chip contained several side chambers, and only sperm swimming into the side chambers were treated as attracted to chemotactants (Fig. 4e). They were tested for sperm motility on a chip made up of three different gels (1% agarose, 8% gelatin, and a hybrid 1% agarose/8% gelatin). Finally, a hydrogel of 8% gelatin and 1% agarose proved optimal due to its biocompatibility and availability to work at relevant temperatures. Using their flow-free device, they

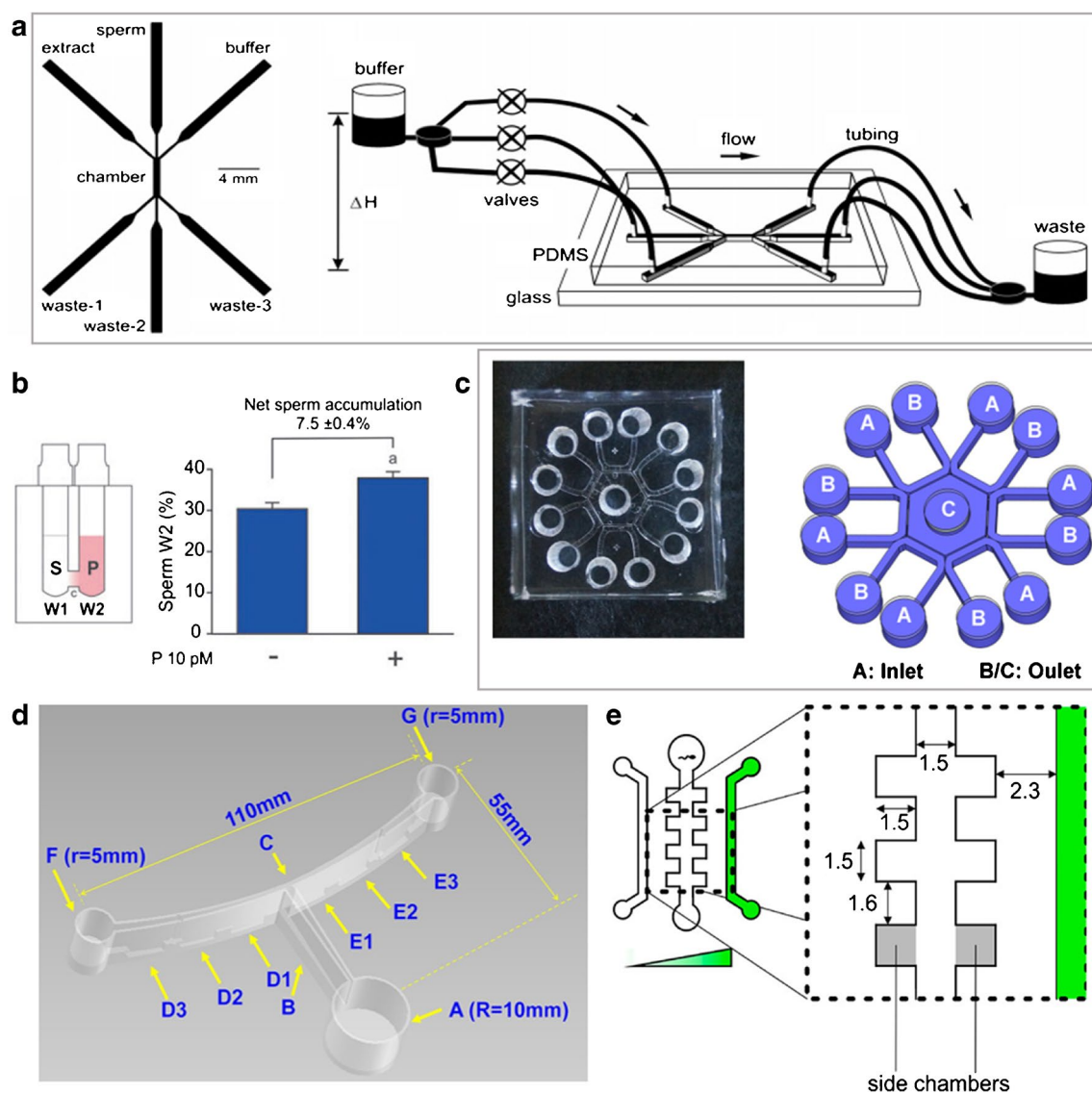


**Fig. 4** Microfluidic chip system for sperm selection based on chemotaxis. **a** Schematic of the microfluidic device for chemotaxis assays and schematic of the microfluidic device with fluid control. Reproduced with permission [33], Copyright © 2006, ACS Publishing. **b** Schematic representation of the sperm selection assay (SSA) based on chemotaxis of progesterone gradients and percentage of sperm accumulation in W2 after SSA with or without progesterone. Reproduced with permission [35], Copyright © 2013, OUP Publishing. **c** Actual photograph and schematic illustration of diffusion-based microfluidic for generating various concentrations of chemotaxis.

Pool A and Pool B/C represent the inlets and outlets of the channels, respectively. Liquid level in Pool A is higher than that in both Pool B/C. Reproduced with permission [48], Copyright © 2015, PLOS ONE Publishing. **d** Schematic of distance-progesterone-combined selection device mimicking human female reproductive tract to study chemotaxis. Reproduced with permission [36], Copyright © 2018, BMC Publishing. **e** Schematic of flow-free chip design based on hybrid hydrogel. Reproduced with permission [37], Copyright © 2020, ACS Publishing

found that sperm were attracted to the progesterone gradient in the physiological range and showed higher chemotaxis ratio (the number of cells directed to the chemoattractant divided by the number of cells that have swum in the opposite direction) than other studies.

There are various analytical methods available for the study of sperm chemotaxis, but the research tools used in these experiments generally lack the ability to generate

stable, controllable, and reproducible concentration gradients. Compared with conventional devices, it is easier to establish stable and controllable concentration gradients in microfluidic chips. Gradient generators can be divided into flow-based chips and flow-free chips [60]. The concentration gradients generated in flow-based devices are stable and persistent, but fluid flow can greatly affect sperm motility [54, 61]. In flow-free devices, the concentration gradient is

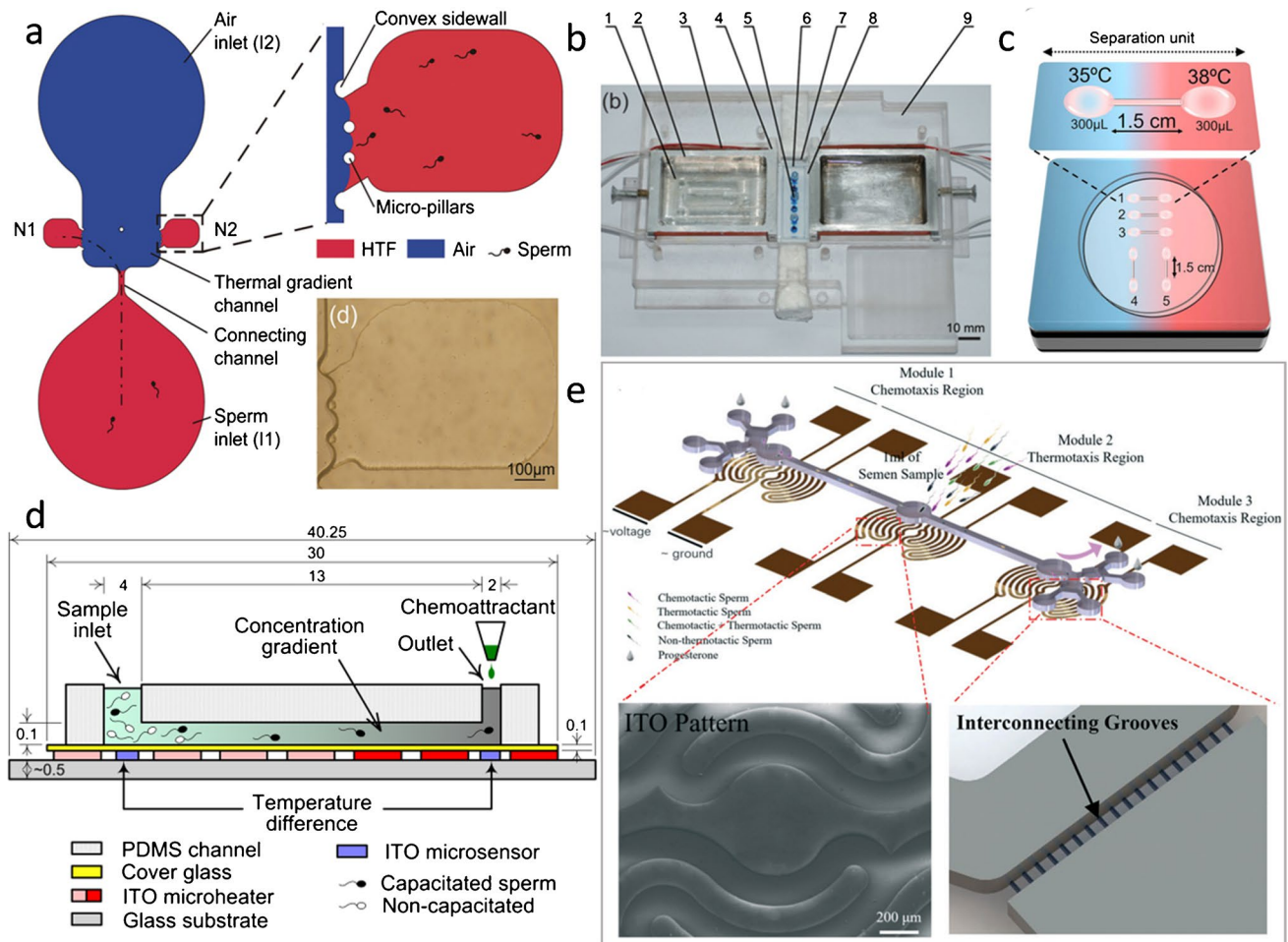


**Fig. 5** Microfluidic chip system for sperm selection based on thermotaxis and the microfluidic chip integrating a comprehensive screening of sperm motility, chemotaxis, and thermotaxis. **(a–b)** Construction of a microfluidic device for human sperm thermotaxis assay based on interface valve closure and detailed illustration of the right branch after interfacial valve closure. **(b)** Top view of the temperature gradient control system. The numbers indicate: 1- glycerol, 2- aluminum alloy tank, 3- resistive heater, 4- thermistor, 5- microfluidic channel, 6- PDMS upper layer, 7- glass lower layer, 8- chip positioning chamber, and 9- PMMA case. Reproduced with permission [38], Copyright © 2014, AIP Publishing. **(c)** Thermotaxis sperm selection assay to improve ICSI results. In the in vitro thermotaxis assay, sperm were loaded in one

drop of medium at one temperature and then migrated to another drop at a high temperature connected by a capillary tube. Reproduced with permission [39], Copyright © 2018, Springer Publishing. **(d)** Schematic diagram of the bioenvironmental mimetic integrated system for analysis of motile sperm. Reproduced with permission [40], Copyright © 2018, ELSEVIER Publishing. **(e)** Schematic view of the fully integrated biomimetic microfluidic device for evaluation of sperm response to thermotaxis and chemotaxis. Module 2 is used to test thermotaxis, and Modules 1 and 3 are used to test chemotaxis. The yellow layer is an ITO pattern, used as a microheater to establish the temperature gradient. Reproduced with permission [41], Copyright © 2021, RSC Publishing

mainly formed based on molecular diffusion, and most of these chips are fabricated by hydrogels [37, 62, 63]. However, the beating of the sperm flagella may be limited due to the viscosity of the hydrogel.

Thermotaxis is the ability of the selected sperm to change their swimming direction at higher temperatures. Sperm reaching the uterine isthmus can determine the location of the egg and move in that direction by sensing the temperature gradient between the uterus and the oviduct. This mechanism was observed in capacitated human sperm for a temperature difference of 0.5°C [38]. The first microfluidic

device used to study sperm thermotaxis (Fig. 5a, b) was reported. The microfluidic device used a gas–liquid interface valve to achieve sperm capture through the implementation of a slow positive flow at air inlet I2. Then, air was used to transfer heat in the temperature control system to form a temperature gradient, and the heating controller changed the temperature at 1.3°C intervals. Using this design, they successfully showed the thermotaxis of about 5.7–10.6% of the motile sperm in the temperature range of 34.0–38.3°C. Pérez-Cerezales et al. [39] demonstrated a microfluidic system for improving ICSI outcomes by sperm selection

through thermotaxis (Fig. 5c). They detected the transfer of spermatozoa through a capillary tube connecting two drops of medium, and between these media, the temperature gradient was 3°C, ranging from 35°C to 38°C. They selected sperm that migrated from 35 to 38°C and demonstrated that they exhibited high motility, better DNA integrity, and less chromatin compaction. More importantly, the mouse sperm selected by thermotaxis had better fertilization outcomes through ICSI.

In vivo, the movement of moving sperm reaching the isthmus is facilitated by the flow of tubal fluid and the temperature gradient between the uterine isthmus and the ampulla of the fallopian tube. When fertile sperm approaches the area of the fallopian tube where the egg is located, the concentration gradient of the chemoattractant is detected and then shows chemotaxis towards the egg [39]. Thus, if the sperm is selected in a combination of thermotaxis and chemotaxis, it will closely resemble the selection process in the real in vivo environment, and provides a means to select better spermatozoa for ICSI. Ko et al. developed a microfluidic device with the goal of analyzing sperm migration under conditions that closely mimic the actual fertilization process [40]. The microfluidic device of this system consisted of a sperm migration microchannel chip and an underlying microheater glass substrate underneath (Fig. 5d). Straight channels were utilized to create linear chemoattractant concentrations and temperature gradients. Microheaters, capable of maintaining different temperatures, were positioned beneath the inlet and outlet side channels to generate a linear temperature gradient. Their analysis shows that utilizing a combination of thermotaxis and chemotaxis is more advantageous than using only one type of motility to attract motile sperm. Very recently, Yan et al. [41] developed a fully integrated biomimetic microfluidic system, considering a comprehensive screening of sperm motility, chemotaxis, and thermotaxis. They established a changing gradient environment to analyze differences in motility and motility parameters of functional sperm, thus exploiting thermotaxis and chemotaxis to improve the performance of sperm selection. The device comprised three layers; a microarray for sperm evaluation, an indium tin oxide (ITO) microheater that is used to create a linear temperature gradient, and a printed circuit board (PCB) to connect a DC current supply (Fig. 5e), enabling four simultaneously integrated thermal experiments and two chemotaxis experiments on a single chip. Furthermore, they narrowed the optimal range of temperature gradients for thermotaxis to between 0.014°C/mm and 0.010°C/mm and statistically demonstrated that thermotaxis and chemotaxis responses are not linked.

In the context of clinical applications, both sperm thermotaxis and chemotaxis show promising implications as selection methods for ARTs. Biomimetic microfluidic devices that can simultaneously test thermotaxis and chemotaxis

reactions can better mimic natural sperm selection in vivo, thus significantly improving fertility and embryo quality. These devices are expected to be useful tools for the study of mammalian sperm migration and the improvement of ICSI. However, the controversial question is whether they are worthy of application to the design of microfluidic systems for sperm isolation purposes. Moreover, they require a highly controlled microenvironment, which makes them complicated and expensive. Such research is still in its infancy, and chips that are easier to manufacture and mass-produce are still yet to be developed. Whether such chips really effectively improve fertilization rates or embryo development, or just complicate everything, still requires more clinical trials to determine.

## IVF on a chip

The advancement in IVF is perhaps the most exciting scientific development in infertility treatment. It involves the fertilization and culture of sperm and oocytes under special laboratory conditions. Since the first successful IVF in 1978, which resulted in a live birth [49], IVF has changed the way a significant proportion of humans reproduce. Traditional IVF techniques have to overcome the manipulation of multiple oocytes in continuous fluid channels to prevent the contamination of biological reactions. Compared with traditional technology, the greatest advantage of the microfluidic-based IVF chip is that it can reduce the occurrence of polyspermy [64]. Unlike microdroplet techniques in static tubes or culture dishes, the oocytes can be exposed to only a few selected sperm in a microfluidic device. To achieve this goal, the oocyte localization is the primary concern. Most of the currently reported IVF chips use geometric constraints to fix the oocytes in the microfluidic space to ultimately achieve sperm and egg binding.

Clark et al. leveraged a raised structure to locate a pig oocyte on the main channel of the chip [64], and on the other side injected the sperm to complete the fertilization effect. Then, the fertilized egg was cultured via continuously changing the medium to observe the fertilization status and the development process of the fertilized egg (Fig. 6a). The results showed that the incidence of multi-sperm-penetration fertilized pig oocytes in this device was significantly lower than that of the traditional microdroplet system ( $p < 0.05$ ). This was also the case for the sperm penetration rate, male pronucleus formation rate, subsequent cleavage rate, and blastocyst formation rate. Then, a microchannel three-dimensional barrier gate structure [65] was designed to localize mouse oocytes for fertilization and subsequent culture (Fig. 6b). The results showed that when the sperm concentration was reduced to  $2\text{--}8 \times 10^4$  cells/mL (namely, the total number of sperm was 1000–4000), the fertilization

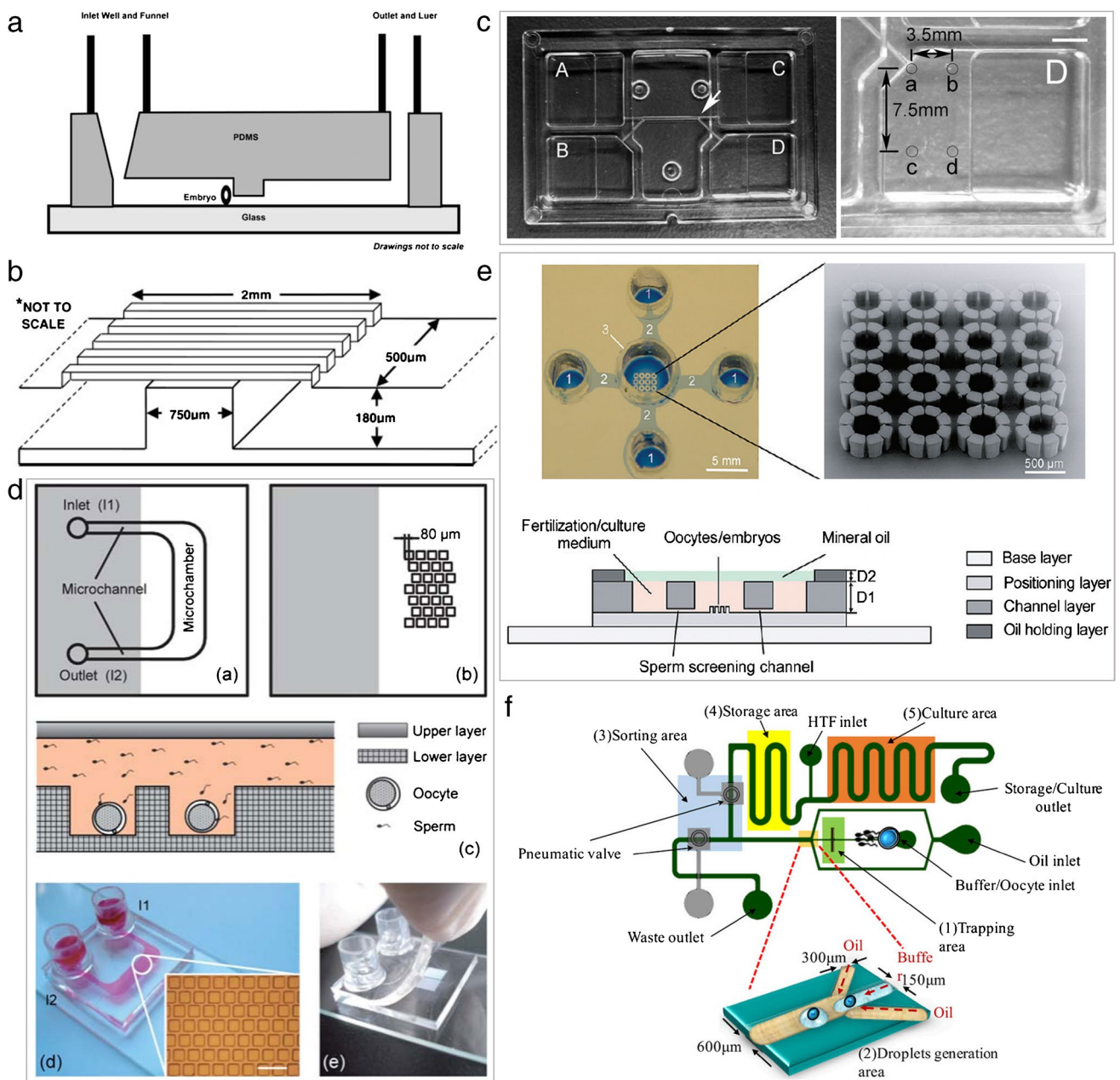


**Fig. 6** Various microfluidic chips for in vitro fertilization. **a** The microchannel design recapitulates the in vivo function. The microchannel routes the sperm to the “parked” oocyte. Reproduced with permission [64], Copyright © 2005, RSC Publishing. **b** Microchannel gate system allows free flow of media and sperm along channel course without passage of oocytes. Reproduced with permission [65], Copyright © 2006, OUP Publishing. **c** A microfluidic device combining a microfluidic sperm sorter with the in vitro fertilization. Photographs of the microfluidic sperm sorter. Micro-streams of semen from chamber A and medium flow from chamber B together, side-by-side in a laminar fashion, and then exit to chambers C and D, respectively

(where oocytes were placed). Reproduced with permission [66], Copyright © 2010, ELSEVIER Publishing. **d** A microwell-structured microfluidic device for oocyte trapping, in vitro fertilization, and embryo culture. Reproduced with permission [67], Copyright © 2010, RSC Publishing. **e** A microfluidic chip that integrates oocyte localization, sperm screening, fertilization, medium replacement, and embryo culture. Reproduced with permission [68], Copyright © 2011, ACS Publishing. **f** Structural diagram of droplet dielectrophoresis (DEP) microfluidic biochip. The size of the chip is 47.72mm × 29.84mm. Reproduced with permission [69], Copyright © 2018, MDPI Publishing

rate in the microchannel (27%) was significantly higher than that in the conventional group (10%). There was no difference in fertilization rate between the conventional

group ( $1 \times 10^6$  cells/mL) and microchannel group. Moreover, the IVF process was integrated on a laminar effect sperm viability screening chip [66] to effectively reduce

multi-sperm penetration of oocyte in pigs (Fig. 6c). There was a significant difference in sperm concentration at A–D of the collection pool [ $(575.0 \pm 56.3) \times 10^4$  cells/mL  $\sim$   $(0.8 \pm 0.5) \times 10^4$  cells/mL]. There was no significant difference in the sperm penetration rate after 8 h of culture when 8–10 egg cells were placed in B, C, and D, respectively. However, there was a significant difference in fertilization rate of single sperm, which was  $(12.5 \pm 4.8)\%$ ,  $(53.1 \pm 6.0)\%$ , and  $(41.9 \pm 2.8)\%$ , respectively. Finally, 30 to 40 denuded oocytes were placed at point c in chamber D of MFSS, exposed to flowing sperm for 5 min, then cultured in fresh decaffeinated medium for 8 h. The result showed that in the MFSS-IVF system, the normal fertilization index (the ratio of single sperm oocytes to the number of detected oocytes;  $37.5 \pm 4.0\%$ ) was higher than that of standard IVF and transient IVF the fertilization index ( $22.2 \pm 2.8$  and  $18.9 \pm 2.7\%$ , respectively). Moreover, the developmental ability of fertilized eggs (blastocyst formation) in the MFSS-IVF system was higher than in either standard or transient IVF. The results showed that the location and quantity of oocytes affected the fertilization efficiency, and the co-culture was beneficial to the formation of blastocyst and monospermy.

A two-layer microfluidic device was designed that was integrated with the function of the capture of individual oocytes, in situ insemination, culture medium alteration, and embryo culture (Fig. 6d) [67]. The first layer consisted of microchannels and micro-compartments, and the second layer included a micropore array to capture and preserve oocytes. The effectiveness of different micropore depths in oocyte capture and debris clearance was compared by computational modeling and flow cleaning experiments. The results indicated that a final depth of 200  $\mu$ m was the most effective. This microwell array has a comparable fertilization rate to traditional droplet-dish techniques, and has the potential to simplify the processing and manipulation of oocytes. This method allows for rapid and convenient fluid-change operations, and can track the development of individual embryos. This facilitates the observation of embryo development and the selection of healthy embryos for clinical use. Although the above devices have successfully combined sperm screening with fertilization steps and achieved some results, there is still significant disparity with the complete IVF system. Therefore, a novel micro-device [68] was reported that integrated every step of IVF, including oocyte localization, sperm screening, fertilization, medium replacement, and embryo culture (Fig. 6e). Oocytes can be individually positioned in a  $4 \times 4$  array of octacolumn units. Four symmetric straight channels intersect with the oocyte localization region, enabling efficient selection of motile sperm and facilitating rapid replacement of the medium. The fertilization process and early embryonic development of individual fertilized eggs were recorded and analyzed using in situ

fluorescent staining. By the screening channels, the sperm motility of mice increased from  $60.8 \pm 3.4\%$  to  $96.1 \pm 1.9\%$ , and the embryo growth rate and blastocyst formation were similar to those of the conventional dish group. The IVF lab-on-a-chip provides a highly integrated platform for human IVF and animal embryo preparation to greatly reduce the adverse effects of manual manipulation on cells, with high potential for basic research and future clinical applications.

Electric fields are also used to detect and manipulate sperm and oocytes. The results showed that the oocytes treated with electrotherapy had better developmental potential than the untreated oocytes [70]. Huang et al. [69] developed a laboratory-on-chip (LOC) system for controlling sperm and oocyte fertilization. They used a droplet-based biochip, leveraging the dielectrophoresis (DEP) effect and microfluidic system to transport, classify and store oocytes, sperm and embryos. The microfluidic chip can be divided into four main parts (Fig. 6f): (1) Trapping area: The oocytes were manipulated by positive DEP force, and sperm were concentrated on indium tin oxide (ITO) electrode. (2) Droplet generation: Flow focusing design was used to generate emulsion microfluids (approximately 100 nl volume) in individual oocytes. (3) Sorting area: A pneumatic valve was used to classify the droplets of fertilized eggs. (4) Storage area: Droplet storage for culture. According to the observation results, the local sperm concentration increased by 20 to 40 times compared with the original sperm concentration, and the fertilization rate rose with the increase in the sperm–oocyte ratio. When the sperm–oocyte ratio was 500, the fertilization rate and the blastocyst rate of DEP microfluidic IVF chip were 39.4% and 33.3%, respectively, and when the sperm–oocyte ratio was 2000, the fertilization rate and the blastocyst rate of the DEP microfluidic IVF chip were 50.2% and 25.1%, respectively. Compared to the traditional method of IVF, the fertilization rate of DEP microfluidic IVF increased by 5%, and even more than 20% developed to blastocyst stage.

Similar to IVF, ICSI is the treatment technique of choice for many infertile male patients (with a global implementation rate of approximately 66%) [7, 71]. The success of ICSI and sperm–oocyte fertilization depends considerably on the selection of sperm with high DNA and viability from damaged and nonviable sperm and fragments [72, 73]. Microfluidic devices have been proven to provide higher accuracy in ICSI therapy compared to human technicians. They are capable of selecting the best candidate sperm based on quality and fertilization potential, as well as reducing treatment time by increasing sperm concentration in poor-quality semen samples [24, 74]. However, the method is relatively expensive and relies heavily on artificial manipulation. There is also a risk of oocyte lysis when the needle is inserted into the oocyte. In the future,

there is an expectation for the development and utilization of more economical and automated ICSI, combined with microfluidic technologies.

## Summary, challenges, and future prospects

The labor-intensive method of sperm screening can result in low purity and DNA damage in sperm cells, which in turn limits the success rate of ICSI. Also, traditional IVF processes are still far from replicating the real fertilization process in the human microenvironment. Moreover, traditional methods with their process complexity, error-prone, costly, and highly dependent on technical proficiency, are difficult and unaffordable for couples living in remote and resource-limited areas. As a result, public attention is turning to miniaturized, integrated, automated, and low production-cost microfluidic chips. Microfluidics can replace large traditional laboratory tests that require large laboratory settings, high cost and manpower, and perform automated multiple tests on a small scale. Thus, microfluidics has great potential in the future of biomedicine, and has broad applications in ARTs. This paper highlights the significant contribution of microfluidic technology in isolating progressively motile sperm from raw semen to enhance ICSI outcomes, optimize the IVF process, and improve its success rate. For sperm screening, we analyzed and discussed the microchannel screening techniques, laminar effect screening techniques, rheology screening techniques, chemotaxis screening techniques, and thermotactic sperm screening techniques. These passive sperm sorting techniques obviously raise the DNA quality and motility of sperm, which in turn improve the ARTs and especially ICSI outcomes. In terms of IVF, unlike static tubes or droplets, microfluidic IVF requires a lower sperm concentration. Oocytes are exposed to fewer sperm in a low working volume microfluidic device, thus reducing the possibility of polyzoospermia. Furthermore, the advanced integration of microfluidic chips enables the development of an "in vitro fertilization lab chip" that combines various functions such as sperm motility screening, oocyte positioning, IVF, fluid exchange, early embryo culture, embryo tracking, and in situ staining. The application of microfluidics can be integrated into all stages of embryo production, starting with the sorting of sperm, peeling of oocytes, continued fertilization, embryo culture and cryopreservation of embryos. The development of multifunctional microfluidics IVF systems may be driven by advances in 3D printing technology [75, 76], organ on the chip [77–81], and novel material [82, 83]. In addition, there are relatively few relevant studies on the selection, culture, and quality evaluation of oocytes [84–87]. If the oocyte processing equipment can be combined with the sperm screening equipment, it will provide a broader prospect for the development of ARTs.

The full potential and possibilities of microfluidics in ARTs are endless.

Despite the many unique advantages of microfluidic technology in the field of sperm screening and IVF, which indicates significant commercial potential, further research is needed to confirm the reliability and effectiveness of its clinical applications, and challenges and limitations remain (Table 2). Firstly, most current microfluidic devices still require external pumps, pipes, and connectors for setup. These external components can make it difficult to parallelize multiple chips, limiting the overall throughput of the chips. They can also cause issues during transport and storage. Secondly, most microfluidic devices used for sperm sorting are manufactured using PDMS. However, the high cost of PDMS devices makes large-scale production economically unfeasible. More importantly, this material has potential negative effects on cellular studies at the microscale, such as deformation, medium evaporation, molecular absorption, leaching of non-cross-linked oligomers, and hydrophobic recovery [88]. The use of more cost-effective materials, such as thermoplastics [89], may be a reasonable solution. Microprocessing, hot embossing, and 3D printing are the best alternatives to the lithography technology used to build thermoplastic microchips [90, 91]. Thirdly, the flexibility and diversity of microfluidic designs can also lead to a lack of reproducibility and standardization. The manufacturing of these platforms involves infrastructure-intensive manufacturing methods and lacks capacity for mass production. Moreover, its complexity raises the threshold for consumer adoption for a large majority of users. Additionally, the commercialization based on clinical implementation is a great challenge in the future. It is always difficult to transfer the fruits of microfluidic chips on laboratory platforms into the consumer market. Although there have been a few commercially available products developed for semen analysis by using paper-based microfluidics, such as SpermCheck and FertilMARQ [92, 93], the process is time-intensive and the assessment results can be influenced by the intrinsic subjectivity of different observers. More importantly, there is a lack of adequate quantitative techniques for conducting thorough analysis of semen, while other powerful microfluidic techniques for assessing sperm motility and concentration have not yet been commercialized [94]. The problem lies in the limited clinical applicability—as it focuses only on proof-of-concept experiments and ignores additional clinical steps, including further sample processing and material transfer—and the lack of commercial follow-up analysis [95]. At present, most microfluidic devices used for sperm sorting or IVF only perform well in laboratories, whereas researchers may not be able to consider the commercial application of the final products. For example, the quality and quantity of sperm samples

**Table 2** Advantages and limitations of current microfluidic technologies, and possible solutions

|   | Advantages of the microfluidic technology  | Challenges of current microfluidic chips   | Possible solution  |
|---|--|--|--|
| Sperm selection by microchannel               | <ul style="list-style-type: none"> <li>- Selects sperm of fish (not following any physical or chemical cues to reach the egg)</li> <li>- Structure is simple and easy to operate</li> </ul>  | <ul style="list-style-type: none"> <li>- A comprehensive assessment of the sperm quality could not be achieved</li> <li>- Clogging and air bubble issues</li> <li>- High cost of fabrication</li> </ul>  | <ul style="list-style-type: none"> <li>- Combine with other sorting mechanisms, such as thermotaxis and chemotaxis</li> </ul>  |
| Sperm selection by laminar flow               | <ul style="list-style-type: none"> <li>- Effectively reduces the DNA damage</li> <li>- Works with small sample volumes</li> </ul>  | <ul style="list-style-type: none"> <li>- Limited throughput</li> <li>- Requires external pumps, pipes, and connectors</li> <li>- Sperm recovery is less efficient</li> <li>- Clogging and air bubble issues</li> </ul>                             | <ul style="list-style-type: none"> <li>- Use hydrostatic pressure instead of the external pump</li> <li>- Set up multiple channels or increase the channel width to increase the efficiency</li> </ul> |
| Sperm selection by rheology                   | <ul style="list-style-type: none"> <li>- Effectively reduces the DNA damage</li> <li>- High-throughput</li> <li>- Selects functional subpopulations of specific movement patterns</li> </ul>   | <ul style="list-style-type: none"> <li>- Requires external pumps, pipes, and connectors</li> <li>- The diversity of designs makes it difficult to standardize</li> <li>- Clogging and air bubble issues</li> </ul>                                 | <ul style="list-style-type: none"> <li>- Use hydrostatic pressure instead of the external pump</li> </ul>  |
| Sperm selection by chemotaxis and thermotaxis | <ul style="list-style-type: none"> <li>- Effective selection of capacitated sperm</li> <li>- Better simulation of the <i>in vivo</i> environment</li> </ul>  | <ul style="list-style-type: none"> <li>- Difficult to control</li> <li>- Sperm recovery is low (~10%)</li> <li>- Time-consuming</li> <li>- Clogging and air bubble issues</li> <li>- High cost of fabrication</li> </ul>                           | <ul style="list-style-type: none"> <li>- Use a microheater (ITO)</li> <li>- Perform multiple parallel experiments on one chip</li> </ul>   |
| IVF   | <ul style="list-style-type: none"> <li>- Oocytes only need to be exposed to a few sperm to prevent polyspermatation</li> <li>- Local flow regulation and geometry adjustment to improve the success rate</li> <li>- Regulates the microenvironment for optimal embryo culture</li> </ul> | <ul style="list-style-type: none"> <li>- Limited throughput</li> <li>- Requires external pumps, pipes, and connectors</li> <li>- Difficulty in removing embryos from the microfluidic channel</li> <li>- Clogging and air bubble issues</li> </ul> | <ul style="list-style-type: none"> <li>- Use micropumps and microvalves to control the on-chip flow operation</li> <li>- Combine with machine learning or artificial intelligence</li> </ul>           |



selected in some microfluidic experiments are better than the actual situation. Most infertile patients may produce fewer or less viable sperm. Perhaps researchers and developers need to collaborate more closely with clinicians to expedite the application of microfluidic technology in clinical cases. This would involve obtaining safety and pre-market approval from relevant regulatory authorities, such as the US Food and Drug Administration (FDA), in order to assess the commercial potential of these technologies and address the numerous challenges associated with infertility.

Taken together, the evidence shows that although prominent advances have been made in the field of ART medicine, infertility continues to affect couples worldwide. Semen analysis tests and the most common methods for classifying sperm are still expensive, time-consuming, and inconvenient. Microfluidic devices are able to overcome the limitations of conventional methods to provide simple, economical, and convenient solutions for semen analysis, high-quality sperm selection, and IVF. However, beyond device development and preliminary clinical testing, these technologies lack extensive clinical practice and have not yet reached the commercialization stage. We also suggest that different methods be combined with microfluidic technology, leveraging artificial intelligence, cloud learning or machine learning methods [96], to fully realize the tremendous potential of microfluidic technology. This will accelerate the commercial deployment and final clinical application, addressing the challenges of global fertility.

**Funding** This work was supported by the National Natural Science Foundation of China (32201179), Guangdong Basic and Applied Basic Research Foundation (2020A1515110126 and 2021A1515010130) and the Fundamental Research Funds for the Central Universities (N2319005).

## Declarations

**Conflicts of interests** The authors declare no competing interests.

## References

- Zegers-Hochschild F, Adamson GD, de Mouzon J, Ishihara O, Mansour R, Nygren K, et al. International Committee for Monitoring Assisted Reproductive Technology (ICMART) and the World Health Organization (WHO) revised glossary of ART terminology, 2009. *Fertility and Sterility*. 2009;92(5):1520–4.
- Cox CM, Thoma ME, Tchangelova N, Mburu G, Bornstein MJ, Johnson CL, et al. Infertility prevalence and the methods of estimation from 1990 to 2021: a systematic review and meta-analysis. *Hum Reprod. Open*. 2022;2022(4):hoac051.
- Kumar N, Singh AK. Trends of male factor infertility, an important cause of infertility: A review of literature. *J Hum Reprod Sci*. 2015;8(4):191–6.
- Barak S, Baker HWG. *Clinical Management of Male Infertility*. Endotext. South Dartmouth (MA): MDTText.com, Inc.; 2000.
- Tasoglu S, Safaee H, Zhang X, Kingsley JL, Catalano PN, Gurkan UA, et al. Exhaustion of racing sperm in nature-mimicking microfluidic channels during sorting. *Small*. 2013;9(20):3374–84.
- Dickey RP. The relative contribution of assisted reproductive technologies and ovulation induction to multiple births in the United States 5 years after the Society for Assisted Reproductive Technology/American Society for Reproductive Medicine recommendation to limit the number of embryos transferred. *Fertility and Sterility*. 2007;88(6):1554–61.
- Palermo G, Joris H, Devroey P, Van Steirteghem AC. Pregnancies after intracytoplasmic injection of single spermatozoon into an oocyte. *Lancet*. 1992;340(8810):17–8.
- Jin X, Wang G, Liu S, Zhang J, Zeng F, Qiu Y, et al. Survey of the situation of infertile women seeking in vitro fertilization treatment in China. *Biomed Res Int*. 2013;2013:179098.
- Sunderam S, Kissin DM, Crawford SB, Folger SG, Boulet SL, Warner L, et al. Assisted Reproductive Technology Surveillance - United States, 2015. *MMWR Surveill Summ*. 2018;67(3):1–28.
- Kashaninejad N, Shiddiky MJA, Nguyen NT. Advances in Microfluidics-Based Assisted Reproductive Technology: From Sperm Sorter to Reproductive System-on-a-Chip. *Adv Biosyst*. 2018;2(3):1700197.
- Said TM, Land JA. Effects of advanced selection methods on sperm quality and ART outcome: a systematic review. *Hum Reprod Update*. 2011;17(6):719–33.
- Simon L, Murphy K, Shamsi MB, Liu L, Emery B, Aston KI, et al. Paternal influence of sperm DNA integrity on early embryonic development. *Hum Reprod*. 2014;29(11):2402–12.
- Sakkas D, Ramalingam M, Garrido N, Barratt CL. Sperm selection in natural conception: what can we learn from Mother Nature to improve assisted reproduction outcomes? *Hum Reprod Update*. 2015;21(6):711–26.
- Rappa KL, Rodriguez HF, Hakkarainen GC, Anchan RM, Mutter GL, Asghar W. Sperm processing for advanced reproductive technologies: Where are we today? *Biotechnol Adv*. 2016;34(5):578–87.
- Akerlöf E, Fredricson B, Gustafsson O, Lundin A, Lunell NO, Nylund L, et al. Comparison between a swim-up and a Percoll gradient technique for the separation of human spermatozoa. *Int J Androl*. 1987;10(5):663–9.
- Matsuura K, Takenami M, Kuroda Y, Hyakutake T, Yanase S, Naruse K. Screening of sperm velocity by fluid mechanical characteristics of a cyclo-olefin polymer microfluidic sperm-sorting device. *Reprod Biomed Online*. 2012;24(1):109–15.
- Figey D, Pinto D. Lab-on-a-chip: a revolution in biological and medical sciences. *Anal Chem*. 2000;72(9):330a–5a.
- Beebe DJ, Mensing GA, Walker GM. Physics and applications of microfluidics in biology. *Annu Rev Biomed Eng*. 2002;4:261–86.
- Swain JE, Lai D, Takayama S, Smith GD. Thinking big by thinking small: application of microfluidic technology to improve ART. *Lab Chip*. 2013;13(7):1213–24.
- Suarez SS, Pacey AA. Sperm transport in the female reproductive tract. *Hum Reprod Update*. 2006;12(1):23–37.
- Nosrati R, Vollmer M, Eamer L, San Gabriel MC, Zeidan K, Zini A, et al. Rapid selection of sperm with high DNA integrity. *Lab Chip*. 2014;14(6):1142–50.
- Eamer L, Vollmer M, Nosrati R, San Gabriel MC, Zeidan K, Zini A, et al. Turning the corner in fertility: high DNA integrity of boundary-following sperm. *Lab Chip*. 2016;16(13):2418–22.
- Chinnasamy T, Kingsley JL, Inci F, Turek PJ, Rosen MP, Behr B, et al. Guidance and Self-Sorting of Active Swimmers: 3D Periodic Arrays Increase Persistence Length of Human Sperm Selecting for the Fittest. *Adv Sci*. 2018; 5(2):1700531.

24. Xiao S, Riordon J, Simchi M, Lagunov A, Hannam T, Jarvi K, et al. FertDish: microfluidic sperm selection-in-a-dish for intracytoplasmic sperm injection. *Lab Chip*. 2021;21(4):775–83.
25. Panigrahi B, Chen CY. Microfluidic retention of progressively motile zebrafish sperms. *Lab Chip*. 2019;19(24):4033–42.
26. Cho BS, Schuster TG, Zhu X, Chang D, Smith GD, Takayama S. Passively driven integrated microfluidic system for separation of motile sperm. *Anal Chem*. 2003;75(7):1671–5.
27. Shirota K, Yotsumoto F, Itoh H, Obama H, Hidaka N, Nakajima K, et al. Separation efficiency of a microfluidic sperm sorter to minimize sperm DNA damage. *Fertility and Sterility*. 2016;105(2):315–21.e1.
28. de Wagenaar B, Berendsen JT, Bomer JG, Olthuis W, van den Berg A, Segerink LI. Microfluidic single sperm entrapment and analysis. *Lab Chip*. 2015;15(5):1294–301.
29. Seo DB, Agca Y, Feng ZC, Critser JK. Development of sorting, aligning, and orienting motile sperm using microfluidic device operated by hydrostatic pressure. *Microfluid Nanofluidics*. 2007;3(5):561–70.
30. Wu JK, Chen PC, Lin YN, Wang CW, Pan LC, Tseng FG. High-throughput flowing upstream sperm sorting in a retarding flow field for human semen analysis. *Analyst*. 2017;142(6):938–44.
31. Nagata MPB, Endo K, Ogata K, Yamanaka K, Egashira J, Katafuchi N, et al. Live births from artificial insemination of microfluidic-sorted bovine spermatozoa characterized by trajectories correlated with fertility. *Proc Natl Acad Sci U S A*. 2018;115(14):E3087–e96.
32. Zaferani M, Cheong SH, Abbaspourrad A. Rheotaxis-based separation of sperm with progressive motility using a microfluidic corral system. *Proc Natl Acad Sci U S A*. 2018;115(33):8272–7.
33. Koyama S, Amarie D, Soini HA, Novotny MV, Jacobson SC. Chemotaxis assays of mouse sperm on microfluidic devices. *Anal Chem*. 2006;78(10):3354–9.
34. Ko YJ, Maeng JH, Lee BC, Lee S, Hwang SY, Ahn Y. Separation of progressive motile sperm from mouse semen using on-chip chemotaxis. *Anal Chem*. 2012;28(1):27–32.
35. Gatica LV, Guidobaldi HA, Montesinos MM, Teves ME, Moreno AI, Uñates DR, et al. Picomolar gradients of progesterone select functional human sperm even in subfertile samples. *Mol Hum Reprod*. 2013;19(9):559–69.
36. Li K, Li R, Ni Y, Sun P, Liu Y, Zhang D, et al. Novel distance-progesterone-combined selection approach improves human sperm quality. *J Transl Med*. 2018;16(1):203.
37. Berendsen JTW, Kruit SA, Atak N, Willink E, Segerink LI. Flow-Free Microfluidic Device for Quantifying Chemotaxis in Spermatozoa. *Anal Chem*. 2020;92(4):3302–6.
38. Li Z, Liu W, Qiu T, Xie L, Chen W, Liu R, et al. The construction of an interfacial valve-based microfluidic chip for thermotaxis evaluation of human sperm. *Biomicrofluidics*. 2014;8(2):024102.
39. Pérez-Cerezales S, Laguna-Barraza R, de Castro AC, Sánchez-Calabuig MJ, Cano-Oliva E, de Castro-Pita FJ, et al. Sperm selection by thermotaxis improves ICSI outcome in mice. *Sci Rep*. 2018;8(1):2902.
40. Ko YJ, Maeng JH, Hwang SY, Ahn Y. Design, Fabrication, and Testing of a Microfluidic Device for Thermotaxis and Chemotaxis Assays of Sperm. *SLAS Technol*. 2018;23(6):507–15.
41. Yan Y, Zhang B, Fu Q, Wu J, Liu R. A fully integrated biomimetic microfluidic device for evaluation of sperm response to thermotaxis and chemotaxis. *Lab Chip*. 2021;21(2):310–8.
42. Kricka LJ, Nozaki O, Heyner S, Garside WT, Wilding P. Applications of a microfabricated device for evaluating sperm function. *Clin Chem*. 1993;39(9):1944–7.
43. Kricka LJ, Faro I, Heyner S, Garside WT, Fitzpatrick G, McKinnon G, et al. Micromachined analytical devices: microchips for semen testing. *J Pharm Biomed Anal*. 1997;15(9–10):1443–7.
44. Xie L, Ma R, Han C, Su K, Zhang Q, Qiu T, et al. Integration of sperm motility and chemotaxis screening with a microchannel-based device. *Clin Chem*. 2010;56(8):1270–8.
45. Denissenko P, Kantsler V, Smith DJ, Kirkman-Brown J. Human spermatozoa migration in microchannels reveals boundary-following navigation. *Proc Natl Acad Sci U S A*. 2012;109(21):8007–10.
46. Yanagimachi R, Cherr G, Matsubara T, Andoh T, Harumi T, Vines C, et al. Sperm attractant in the micropyle region of fish and insect eggs. *Biol Reprod*. 2013;88(2):47.
47. Zaferani M, Palermo GD, Abbaspourrad A. Structures of a microchannel impose fierce competition to select for highly motile sperm. *Sci Adv*. 2019;5(2):eaav2111.
48. Zhang Y, Xiao RR, Yin T, Zou W, Tang Y, Ding J, et al. Generation of Gradients on a Microfluidic Device: Toward a High-Throughput Investigation of Spermatozoa Chemotaxis. *PLoS One*. 2015;10(11):e0142555.
49. Steptoe PC, Edwards RG. Birth after the reimplantation of a human embryo. *Lancet*. 1978;2(8085):366.
50. Weigl BH, Yager P. Microfluidics - Microfluidic diffusion-based separation and detection. *Science*. 1999;283(5400):346–7.
51. Kenis PJ, Ismagilov RF, Whitesides GM. Microfabrication inside capillaries using multiphase laminar flow patterning. *Science*. 1999;285(5424):83–5.
52. Takayama S, Ostuni E, LeDuc P, Naruse K, Ingber DE, Whitesides GM. Subcellular positioning of small molecules. *Nature*. 2001;411(6841):1016.
53. Hyakutake T, Hashimoto Y, Yanase S, Matsuura K, Naruse K. Application of a numerical simulation to improve the separation efficiency of a sperm sorter. *Biomed Microdevices*. 2009;11(1):25–33.
54. Miki K, Clapham DE. Rheotaxis guides mammalian sperm. *Curr Biol*. 2013;23(6):443–52.
55. Chan PJ, Jacobson JD, Corselli JU, Patton WC. A simple zeta method for sperm selection based on membrane charge. *Fertility and Sterility*. 2006;85(2):481–6.
56. Eisenbach M, Giojalas LC. Sperm guidance in mammals - an unpaved road to the egg. *Nat Rev Mol Cell Biol*. 2006;7(4):276–85.
57. Kaupp UB, Kashikar ND, Weyand I. Mechanisms of sperm chemotaxis. *Annu Rev Physiol*. 2008;70:93–117.
58. Oren-Benaroya R, Orvieto R, Gakamsky A, Pinchasov M, Eisenbach M. The sperm chemoattractant secreted from human cumulus cells is progesterone. *Hum Reprod*. 2008;23(10):2339–45.
59. Anderson RA Jr, Feathergill KA, Rawlins RG, Mack SR, Zaneveld LJ. Atrial natriuretic peptide: a chemoattractant of human spermatozoa by a guanylate cyclase-dependent pathway. *Mol Reprod Dev*. 1995;40(3):371–8.
60. Li J, Lin F. Microfluidic devices for studying chemotaxis and electrotaxis. *Trends Cell Biol*. 2011;21(8):489–97.
61. Tung CK, Ardon F, Fiore AG, Suarez SS, Wu M. Cooperative roles of biological flow and surface topography in guiding sperm migration revealed by a microfluidic model. *Lab Chip*. 2014;14(7):1348–56.
62. Srinivasan P, Zervantonakis IK, Kothapalli CR. Synergistic effects of 3D ECM and chemogradients on neurite outgrowth and guidance: a simple modeling and microfluidic framework. *PLoS One*. 2014;9(6):e99640.
63. Cheng SY, Heilman S, Wasserman M, Archer S, Shuler ML, Wu M. A hydrogel-based microfluidic device for the studies of directed cell migration. *Lab Chip*. 2007;7(6):763–9.
64. Clark SG, Haubert K, Beebe DJ, Ferguson CE, Wheeler MB. Reduction of polyspermic penetration using biomimetic microfluidic technology during in vitro fertilization. *Lab Chip*. 2005;5(11):1229–32.
65. Suh RS, Zhu X, Phadke N, Ohl DA, Takayama S, Smith GD. IVF within microfluidic channels requires lower total

- numbers and lower concentrations of sperm. *Hum Reprod.* 2006;21(2):477–83.
66. Sano H, Matsuura K, Naruse K, Funahashi H. Application of a microfluidic sperm sorter to the in-vitro fertilization of porcine oocytes reduced the incidence of polyspermic penetration. *Theriogenology.* 2010;74(5):863–70.
  67. Han C, Zhang Q, Ma R, Xie L, Qiu T, Wang L, et al. Integration of single oocyte trapping, in vitro fertilization and embryo culture in a microwell-structured microfluidic device. *Lab Chip.* 2010;10(21):2848–54.
  68. Ma R, Xie L, Han C, Su K, Qiu T, Wang L, et al. In vitro fertilization on a single-oocyte positioning system integrated with motile sperm selection and early embryo development. *Anal Chem.* 2011;83(8):2964–70.
  69. Huang HY, Lai YL, Yao DJ. Dielectrophoretic Microfluidic Device for in Vitro Fertilization. *Micromachines.* 2018;9(3):135.
  70. Choi W, Kim JS, Lee DH, Lee KK, Koo DB, Park JK. Dielectrophoretic oocyte selection chip for in vitro fertilization. *Biomed Microdevices.* 2008;10(3):337–45.
  71. Dyer S, Chambers GM, de Mouzon J, Nygren KG, Zegers-Hochschild F, Mansour R, et al. International Committee for Monitoring Assisted Reproductive Technologies world report: Assisted Reproductive Technology 2008, 2009 and 2010. *Hum Reprod.* 2016;31(7):1588–609.
  72. Simon L, Lewis SE. Sperm DNA damage or progressive motility: which one is the better predictor of fertilization in vitro? *Syst Biol Reprod Med.* 2011;57(3):133–8.
  73. Elbashir S, Magdi Y, Rashed A, et al. Relationship between sperm progressive motility and DNA integrity in fertile and infertile men. *Middle East Fertil Soc J.* 2018;23(3):195–8.
  74. Matsuura K, Uozumi T, Furuichi T, Sugimoto I, Kodama M, Funahashi H. A microfluidic device to reduce treatment time of intracytoplasmic sperm injection. *Fertility and Sterility.* 2013;99(2):400–7.
  75. Bhattacharjee N, Urrios A, Kanga S, Folch A. The upcoming 3D-printing revolution in microfluidics. *Lab Chip.* 2016;16(10):1720–42.
  76. Nielsen AV, Beauchamp MJ, Nordin GP, Woolley AT. 3D Printed Microfluidics. *Annu Rev Anal Chem.* 2020;13(1):45–65.
  77. Li W-X, Liang G, Yan W, Zhang Q, Wang W, Zhou X, et al. Artificial Uterus on a Microfluidic Chip. *Chinese J Anal Chem.* 2013;41:467–72.
  78. Aziz AUR, Fu M, Deng J, Geng C, Luo Y, Lin B, et al. A Microfluidic Device for Culturing an Encapsulated Ovarian Follicle. *Micromachines.* 2017;8(11):335.
  79. Ferraz MA, Henning HH, Van Dorenmalen KM, Vos PL, Stout TA, Malda J, et al., editors. Use of transwell cell culture and 3-D printing technology to develop an in vitro oviduct model to study bovine fertilization. *Fertil Dev.* 2016; 28:156–156.
  80. Zheng F, Fu F, Cheng Y, Wang C, Zhao Y, Gu Z. Organ-on-a-Chip Systems: Microengineering to Biomimic Living Systems. *Small.* 2016;12(17):2253–82.
  81. Yang Y, Noviana E, Nguyen MP, Geiss BJ, Dandy DS, Henry CS. Paper-Based Microfluidic Devices: Emerging Themes and Applications. *Anal Chem.* 2017;89(1):71–91.
  82. Ren KN, Chen Y, Wu HK. New materials for microfluidics in biology. *Curr Opin Biotechnol.* 2014;25:78–85.
  83. Nielsen JB, Hanson RL, Almughamsi HM, Pang C, Fish TR, Woolley AT. Microfluidics: Innovations in Materials and Their Fabrication and Functionalization. *Anal Chem.* 2020;92(1):150–68.
  84. Angione SL, Oulhen N, Brayboy LM, Tripathi A, Wessel GM. Simple perfusion apparatus for manipulation, tracking, and study of oocytes and embryos. *Fertility and Sterility.* 2015;103(1):281–290.e5.
  85. Weng L, Lee GY, Liu J, Kapur R, Toth TL, Toner M. On-chip oocyte denudation from cumulus-oocyte complexes for assisted reproductive therapy. *Lab Chip.* 2018;18(24):3892–902.
  86. Zeggari R, Wacogne B, Pieralli C, Roux C, Gharbi T. A full micro-fluidic system for single oocyte manipulation including an optical sensor for cell maturity estimation and fertilisation indication. *Sens Actuators B Chem.* 2007;125(2):664–71.
  87. Luo Z, Guven S, Gozen I, Chen P, Tasoglu S, Anchan RM, et al. Deformation of a single mouse oocyte in a constricted microfluidic channel. *Microfluid Nanofluidics.* 2015;19(4):883–90.
  88. Berthier E, Young EW, Beebe D. Engineers are from PDMS-land, Biologists are from Polystyrenia. *Lab Chip.* 2012;12(7):1224–37.
  89. Kang Y, Zou L, Qiu B, Liang X, Sun S, Gao D, et al. Unloading of cryoprotectants from cryoprotectant-loaded cells on a microfluidic platform. *Biomed Microdevices.* 2017;19(2):15.
  90. Berenguel-Alonso M, Sabés-Alsina M, Morató R, Ymberñ O, Rodríguez-Vázquez L, Talló-Parra O, et al. Rapid Prototyping of a Cyclic Olefin Copolymer Microfluidic Device for Automated Oocyte Culturing. *SLAS Technol.* 2017;22(5):507–17.
  91. Gnecco JS, Pensabene V, Li DJ, Ding T, Hui EE, Bruner-Tran KL, et al. Compartmentalized Culture of Perivascular Stroma and Endothelial Cells in a Microfluidic Model of the Human Endometrium. *Ann Biomed Eng.* 2017;45(7):1758–69.
  92. Klotz KL, Coppola MA, Labrecque M, Brugh VM 3rd, Ramsey K, Kim KA, et al. Clinical and consumer trial performance of a sensitive immunodiagnostic home test that qualitatively detects low concentrations of sperm following vasectomy. *J Urol.* 2008;180(6):2569–76.
  93. Coppola MA, Klotz KL, Kim KA, Cho HY, Kang J, Shetty J, et al. SpermCheck Fertility, an immunodiagnostic home test that detects normozoospermia and severe oligozoospermia. *Hum Reprod.* 2010;25(4):853–61.
  94. Brezina PR, Haberl E, Wallach E. At home testing: optimizing management for the infertility physician. *Fertility and Sterility.* 2011;95(6):1867–78.
  95. Volpatti LR, Yetisen AK. Commercialization of microfluidic devices. *Trends Biotechnol.* 2014;32(7):347–50.
  96. You JB, McCallum C, Wang Y, Riordon J, Nosrati R, Sinton D. Machine learning for sperm selection. *Nat Rev Urol.* 2021;18(7):387–403.

**Publisher's note** Springer Nature remains neutral with regard to jurisdictional claims in published maps and institutional affiliations.

Springer Nature or its licensor (e.g. a society or other partner) holds exclusive rights to this article under a publishing agreement with the author(s) or other rightsholder(s); author self-archiving of the accepted manuscript version of this article is solely governed by the terms of such publishing agreement and applicable law.